

Microfabricated vapor preconcentrator for portable ion mobility spectroscopy

Michael Martin^{a,*}, Mark Crain^a, Kevin Walsh^a, R. Andrew McGill^b,
Eric Houser^b, Jennifer Stepnowski^b, Stanley Stepnowski^b,
Huey-Daw Wu^b, Stuart Ross^c

^a University of Louisville, Louisville, KY, United States

^b Naval Research Laboratory, Code 6375, Washington, DC, United States

^c Dstl, Porton Down, Salisbury, UK

Received 28 June 2006; received in revised form 19 March 2007; accepted 20 March 2007

Available online 5 April 2007

Abstract

This paper reports on the design, simulation, fabrication and performance of 6.65 mm × 6.65 mm micromachined vapor preconcentrator devices. The devices are composed of sorbent-coated dual serpentine platinum heaters supported by a 6 μm thick layer of polyimide suspended over a silicon frame. The preconcentrators are designed to allow analyte flow normal to the surface through a 10 × 23 array of 375 μm × 125 μm perforations in the polyimide heater support. This facilitates relatively large airflow through the device while providing intimate contact with the sorbent layer with low pressure drop. In preliminary experiments, the device is demonstrated by interfacing to the front end of a commercial ion mobility spectrometer for trace explosives detection. Samples of 2,4,6-trinitrotoluene from a NESTT (non-hazardous explosives for security training and testing) source were collected on the preconcentrator for 15 min at a concentration adjusted to be just above the detector's noise floor. The results show at least an order of magnitude signal enhancement.

© 2007 Elsevier B.V. All rights reserved.

Keywords: Preconcentrator; Explosives detection; Microheater; Micro-hotplate; Vapor preconcentrator; Ion mobility spectroscopy (IMS)

1. Introduction

Trace detection of illicit materials is an area of increasing importance for survey operations to monitor for the presence of explosives, narcotics, chemical or biological agents, or toxic industrial chemicals. There is a general trend to miniaturize trace detection technologies to allow for their wider utility through possible performance gains (e.g. sensitivity, selectivity, and power requirements), cost benefits, or by opening application areas as a result of the reductions in system size [1–3].

In this work we present the development of a micromachined preconcentrator device. The preconcentrator device is an important subsystem of a trace detector, which can be used to collect and concentrate analyte of interest. After collection, a thermal desorption stage provides a concentrated release of analyte

which can substantially improve the signal to noise ratio at the detector.

A common trace detection system used in bench top and hand-held configurations is the ion mobility spectrometer (IMS) [4–6] (Fig. 1). These devices operate by drawing an air sample into an ionization region where the ionized analyte is accelerated transverse to the source by a uniform electric field in a drift tube. The species are detected as a current generated at the end of the drift region by a Faraday cup. Specific analytes are then identified according to their time-of-flight along the drift tube.

2. Design

In this work, the design of the chemical preconcentrator takes the form of a microfabricated, perforated hotplate that is coated with a sorbent polymer to trap analytes of interest at or near room temperature during the collection phase. At 6.65 mm × 6.65 mm, the dimensions of the heated area are relatively large for MEMS preconcentrators [7–11] to allow for

* Corresponding author. Tel.: +1 502 852 3971.

E-mail address: michael.martin@louisville.edu (M. Martin).

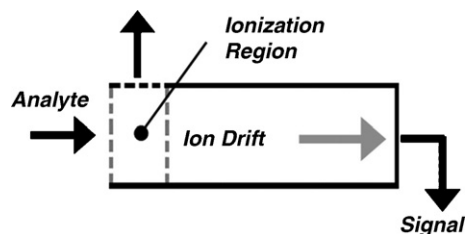


Fig. 1. Basic operating principles for ion mobility spectroscopy.

high flow rate collections and to easily interface to the explosives detector used. These devices differ from the work of Tian and Ruiz [8–11] in that their preconcentrators are designed for quantitative analysis of a broad spectrum of analytes whereas a single CASPAR device is intended only to enhance the detection threshold of a narrow class of analytes; namely organophosphates and nitro-aromatic compounds. Therefore, issues such as breakthrough volume and breadth of analytes are secondary to simply delivering an analyte pulse that is above the detector's noise floor.

The analytes of interest for this work are explosives, and for these preliminary studies the test analyte chosen was 2,4,6-trinitrotoluene (TNT). For TNT, a suitable complimentary functionalized carbosilane sorbent polymer was selected as the preconcentrator coating. The sorbent polymer is a hyper-branched carbosilane with hexafluoroisopropanol functional groups (designated HC), and has been previously demonstrated as a useful sorbent material for hydrogen bond basic analytes such as organophosphates and nitro-aromatics, when used as a coating on chemical sensors [12].

In order to minimize both power consumption and the thermal time constant the heater traces are supported by a thin membrane. Several approaches to heater support were investigated; a $2\ \mu\text{m}$ thick silicon nitride membrane, a $2\ \mu\text{m}$ thick heavily doped p++ silicon layer, and a $6\ \mu\text{m}$ thick polyimide layer. Designs were initially evaluated with a CoventorWareTM finite element analysis (FEA) software package to simulate operational characteristics. The FEA indicated that the highly doped silicon device had the least temperature variation ($<1\%$) but would consume $2.7\ \text{W}$ in order to achieve $120\ ^\circ\text{C}$, the silicon nitride device with platinum heaters would have a temperature variation of $<3\%$ while consuming $0.5\ \text{W}$ to achieve $120\ ^\circ\text{C}$, and that the polyimide device with platinum heaters would have a temperature variation of $<50\%$ and consume $0.12\ \text{W}$ to achieve $120\ ^\circ\text{C}$. In addition, the time required for each design to reach a steady state temperature of $120\ ^\circ\text{C}$ was evaluated. The doped silicon model required up to $1\ \text{s}$, the silicon nitride required only $10\ \text{ms}$, and the polyimide model required $0.25\ \text{s}$ to reach a steady state temperature of $120\ ^\circ\text{C}$. Then, fabrication approaches were evaluated for the three designs. Both the silicon nitride and p++ devices were found to be quite difficult to fabricate and very fragile to handle. We therefore report on only the polyimide membrane design in this paper.

A number of design constraints are imposed on the preconcentrator by this application. The foremost of these are typical considerations for portable sensing, including: low power consumption, small physical footprint, and mechanical robustness. The preconcentrator must also have a short thermal time constant ($10\text{--}100\ \text{ms}$) while reaching a desorption temperature between $100\ ^\circ\text{C}$ and $200\ ^\circ\text{C}$. By minimizing the thermal time constant,

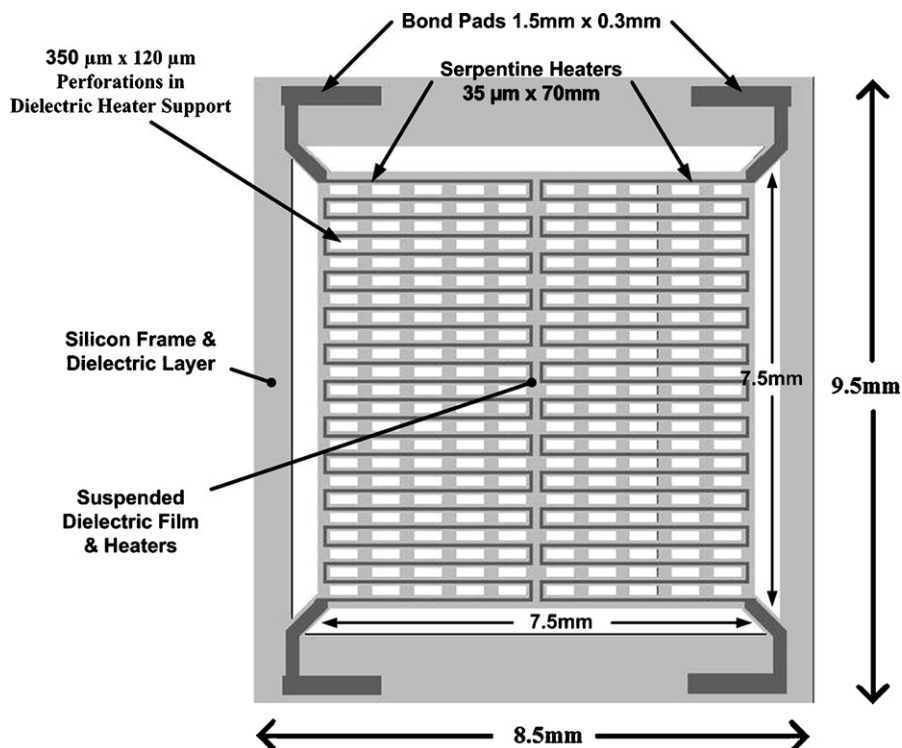


Fig. 2. Basic preconcentrator design.

the analyte desorbed from the preconcentrator arrives at the detector at higher concentrations, effectively enhancing the trace detector system sensitivity. The basic design reported here is depicted in Fig. 2. It features two serpentine platinum heaters that are $35\ \mu\text{m}$ wide and defines an active heated region that is $6.65\ \text{mm} \times 6.65\ \text{mm}$. The platinum heaters are supported by a $6\ \mu\text{m}$ thick layer of polyimide which is perforated by an array of $375\ \mu\text{m} \times 125\ \mu\text{m}$ rectangular openings to produce a $\sim 42\%$ open area fraction within the active region. Relatively large apertures around the outside of the active area serve to thermally isolate it from the cool silicon frame.

3. Fabrication

Devices are fabricated on $525\ \mu\text{m}$ thick (100) 4 in. silicon wafers on which a $0.45\ \mu\text{m}$ thick thermal oxide is grown. The oxide acts as both a masking layer on the back of the devices and as a stop layer at the front for deep reactive ion etching (DRIE). Using VM651 as an adhesion promoter, PI2611 polyimide (both from HD Microsystems, Parlin, NJ) is spin deposited at a spread speed of 500 rpm for 2 s and a spin speed of 3000 rpm for 20 s. After spin coating, the polyimide is first cured on a hotplate in air from $50\ ^\circ\text{C}$ to $200\ ^\circ\text{C}$ at a ramp rate of $2\ ^\circ\text{C}/\text{min}$. Curing is completed in a nitrogen purged tube furnace from $200\ ^\circ\text{C}$ to $400\ ^\circ\text{C}$ at the same ramp rate. Samples are held at $400\ ^\circ\text{C}$ for 1 h after which they are allowed to cool to room temperature at $2\ ^\circ\text{C}/\text{min}$. The final polyimide thickness is $5.6 \pm 0.2\ \mu\text{m}$.

Aluminum is sputtered on the cured polyimide and patterned to act as a masking layer for oxygen plasma etching. The etch step introduces the perforations in the polyimide. After removing the aluminum, photoresist is spin coated and patterned to define the heaters via the lift-off process and a Cr/Pt ($0.05 \pm 0.025\ \mu\text{m}$ and $0.16 \pm 0.03\ \mu\text{m}$ thick, respectively) layer is sputter deposited. The resist is then solvated in acetone to remove metal from the unpatterned regions of the devices. The polished side of the wafer is coated in $7\ \mu\text{m}$ thick positive resist (SPR220 from Shiply, Inc.) in preparation for backside processing and subsequent dicing.

Bulk etch windows for DRIE are opened on the back by spin coating with a $10\ \mu\text{m}$ thick negative resist, OCG SC from OCG Microelectronic Materials, Inc. The resist is exposed after a back to front alignment to produce $8\ \text{mm} \times 8\ \text{mm}$ openings at the back of each die. The exposed oxide is removed in a buffered oxide etch. Before DRIE, the wafer is diced into individual die. The hotplates are plasma etched in groups of up to 16 in order to minimize etch rate variations caused by the large exposed silicon area on the back. This step reduces the time the oxide etch stop is exposed to the plasma.

Each group of die is affixed to a handle wafer that is coated with a $10\ \mu\text{m}$ thick OCG SC-900 negative photoresist. They are attached using silver loaded vacuum grease so that good thermal contact is maintained with the backside helium thermal chuck. While the presence of the photoresist on the top of the handle wafer and downward face of the die impedes cooling of the die during processing, the etch dimensions are large enough that deviations from a 90° wall angle are insignificant.

DRIE is performed in a multiplex ICP (inductively coupled plasma) Etcher from Surface Technology Systems, Plc. for $\sim 4\ \text{h}$ using three platen biases in separate steps. Once the oxide stop layer is exposed, the samples are removed from the DRIE and are post-processed. This is a critical step and can have significant impact on the overall device yield.

Devices are post-processed after DRIE by removing the resist on the back along with the residual Teflon-like coating resulting from the Bosch process. This is achieved in an oxygen plasma generated by a March Plasma Systems, Inc. CS-1701, capacitively coupled reactive ion etcher at 300 mTorr and 400 W for $\sim 15\ \text{min}$. This step allows buffered oxide etchant to effectively wet the stop layer for its removal. Next, the dies are removed from the handle wafer by solvating the positive resist and the thermal vacuum grease on the front with acetone. The devices are frequently contaminated with silver particles from the grease and are therefore cleaned further in an ultrasonic bath of methanol. Once cleaned, the prototype preconcentrator substrates are checked for continuity and mounted in flat pack style packages with a 7 mm diameter hole machined through for ana-

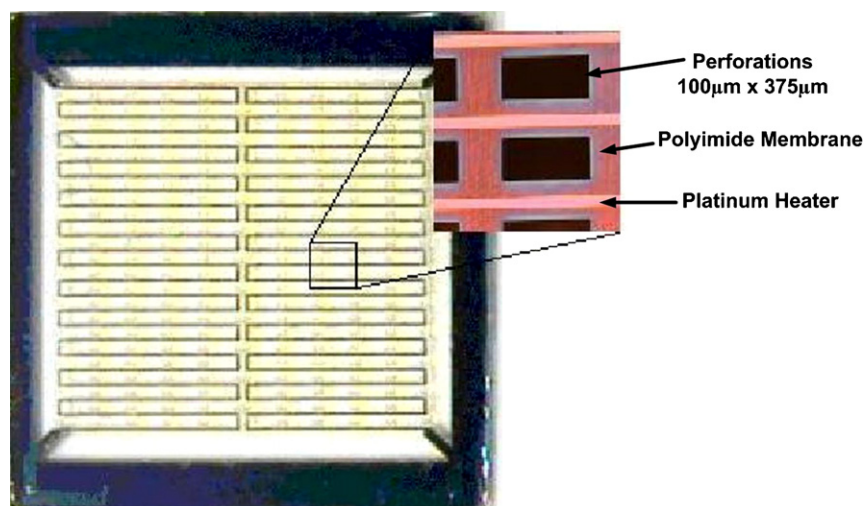


Fig. 3. Micrograph of a $7\ \text{mm} \times 7\ \text{mm}$ prototype with $35\ \mu\text{m}$ wide heaters. The exploded area shows the device structure more clearly.

lyte flow. Fig. 3 is a photograph of a finished 6.65 mm × 6.65 mm prototype before packaging. The overall yield for these devices was ~60%.

Before testing, the sorbent polymer is selectively deposited on the active area using an ink-jet printer. All hotplate chips were first cleaned with chloroform before coating. The ink-jet deposition method uses an ink-jet coating system (Seacoast Science, Inc.). The chip is moved in an incremental fashion using an *X–Y* stage while 0.11% (w/w) solution of polymer HC in chloroform is deposited onto the surface by a computer controlled ink-jet head with an 80 μm orifice. The solvent evaporates leaving a coating of the polymer. This method delivers relatively uniform coatings, allows for accurate control of coating thickness on the hotplate and the ability to coat one or both sides of the hotplate. By examining the films under a light microscope, the coating thickness was determined to be less than 1 μm.

4. Simulation

The finite element analysis (FEA) software, CoventorWare™, was used to model the behavior of the polyimide hotplates. It allows simulation of Joule heating within an electrode and calculation, in three dimensions, of either the transient or steady state thermal distribution.

Simulations are performed by first producing a three-dimensional “solid” model directly from the mask designs. Then material properties are applied to the various volumes. Table 1 summarizes those properties. Given that thin film properties vary significantly from their bulk values, the temperature coefficient of resistance (TCR) for the sputtered platinum heater was measured for 22 separate heaters, averaged together and incorporated as a look-up table in the FEA. Fig. 4 illustrates the TCR along with the corresponding conductivity actually used in the model as a function of temperature.

The simulated geometry is similar to that shown in Fig. 3. It consists of polyimide in light grey and two platinum electrodes in dark grey. The bond pads are not directly incorporated in the model. The geometry has a 35 μm wide heater and a perforation density that produces a 42% open area. The platinum thickness is 0.18 μm and the polyimide is 5.6 μm.

The outside edges of the polyimide are set at 300 K, modeling the heat sink effect of the silicon frame. Effects of convection are modeled in the FEA using a linear convection coefficient. That is, the thermal power (Q_s) flowing from a hotplate surface element to an adjacent air mass, is given by Eq. (1):

$$Q_s = h(T_s - T_a) \quad (1)$$

Table 1
List of material properties used in the FEA model

Material	Platinum	Polyimide [14]	Silicon (100)
Density (kg/m ³)	2.14 × 10 ⁴	1.40 × 10 ³	2.5 × 10 ³
Thermal conductivity (W/m K)	71.6	0.105	148
Specific heat (J/kg K)	133	1089	712
Electric conductivity (S/m)	See Fig. 5	10 ⁻¹⁴	NA

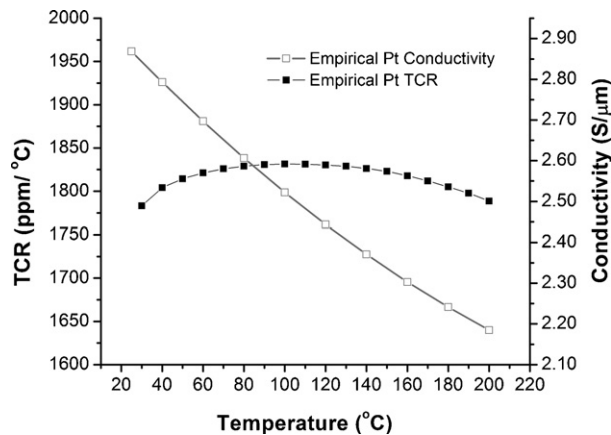


Fig. 4. Empirical TCR and corresponding conductivity as a function temperature as used in the simulation.

where h is the convection coefficient in W/m² K, T_s the temperature of a surface element and T_a is the ambient temperature of the surrounding fluid. For this analysis the convection coefficient for the top surface was set to 125 W/m² K and for the bottom 60 W/m² K [13]. It should be noted that the simulation reflects the situation where the device is heated without flow. Voltages were applied to the end of the heaters.

The peak preconcentrator operating temperature as a function of voltage was investigated from 5 V to 35 V in 5 V increments and compared to experimentally determined values. The data are plotted in Fig. 5. The plot shows good agreement up to 15 V and a slight increasing divergence at higher voltages.

At an operating voltage of 30 V (175 mW), the corresponding average heater temperature was ~120 °C, essentially the target value for the NRL sorbent polymer. The modeled temperature distribution over the hotplate surface at this voltage is shown in Fig. 6. The temperature over the hotplate surface can be seen to vary by as much as 50 °C from the center of heater traces to the polyimide surface between them.

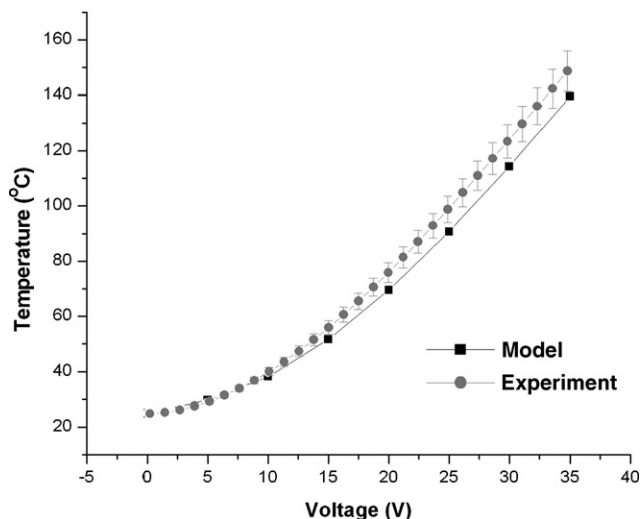


Fig. 5. Graph comparing simulated average temperature in the heater to experimental values as a function of voltage.

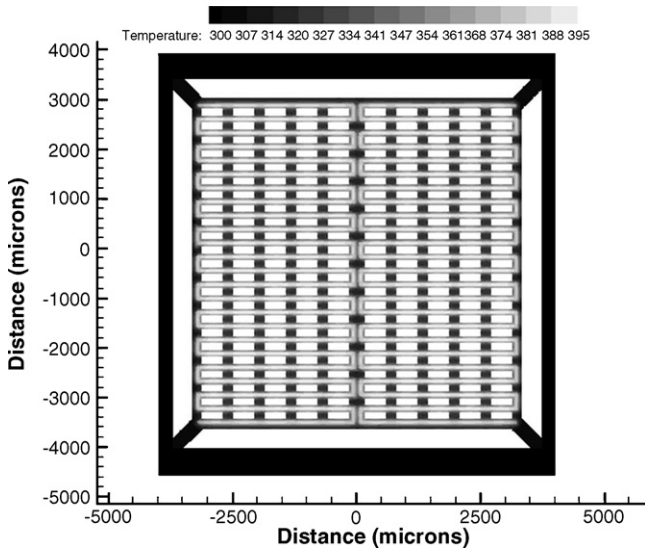


Fig. 6. Simulated two-dimensional temperature distribution for a preconcentrator at 30 V (175 mW) and a peak temperature of 120 °C.

The transient thermal response at 30 V was explored in the model and is presented in Fig. 7 along with the measured transient response. The time constant was determined by fitting the data to an exponential decay given (Eq. (2)):

$$T = T_f + A_1 e^{-t/t'} \quad (2)$$

where T is the temperature as a function of time, T_f the steady state temperature, A_1 a fitting constant and t' is the time constant. The simulation data yields a time constant of 41 ms while the experimental yields 121 m. Due to limitations in the CoventorWare™ package the simulated transient data were generated by using the three-dimensional current density from the steady state solution at 30 V in the transient model. The current and voltage in the transient solution are then treated as constants independent of temperature.

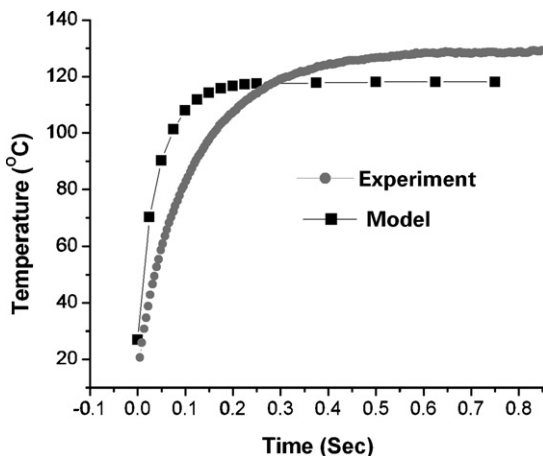


Fig. 7. Simulated and experimental transient response of the preconcentrator after application of 30 V.

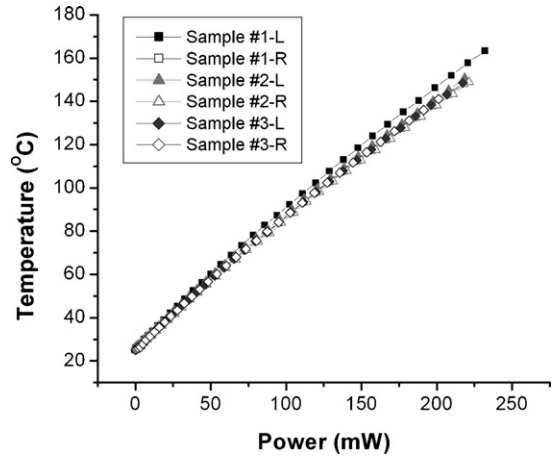


Fig. 8. Calculated temperature verses applied power for six heaters. The R/L designation indicates right or left heater on a given sample.

5. Device electrical performance

Prototypes were initially characterized by measuring resistance as a function of temperature. The resistance measurements were taken with a Keithley 2400 Source Meter and DCP 150 R Precision DC probes in a Summit 11651-6 Thermal Probe Station equipped with a Micro-Chamber. The probes, Micro-Chamber and probe station were from Cascade Microtechnology, Inc. The current for the resistance measurement was fixed to 10 μA to avoid heating the hotplate. The chip was mounted on a thermal chuck (Tempronic Co., Model TP03000A) and the temperature was varied from 25 °C to 200 °C with a Tempronic’s thermal controller.

The temperature versus resistance data were used to determine the temperature coefficient of resistance (TCR) (see Fig. 4). These data were also used as a calibration so that temperature versus power, voltage and time could be found.

Measurements of temperature versus voltage were performed by recording the steady state current of three unpackaged devices using the source meter. The resistance at a given voltage was converted to temperature values using the TCR data. The averaged

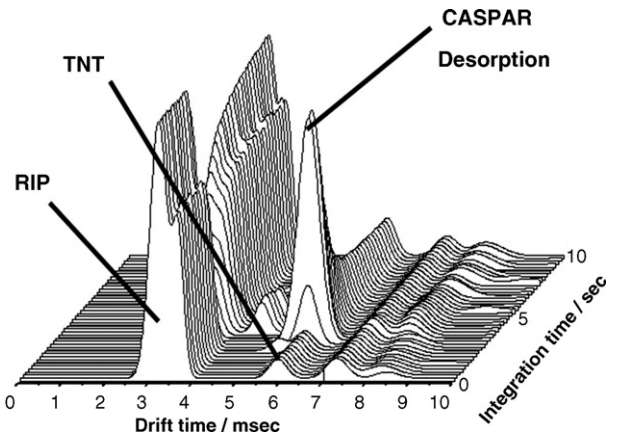


Fig. 9. Vapor Tracer II TNT signal (in arbitrary units) during desorption of a 6.65 mm × 6.65 mm preconcentrator. TNT vapor was collected for 15 min before heating the device.

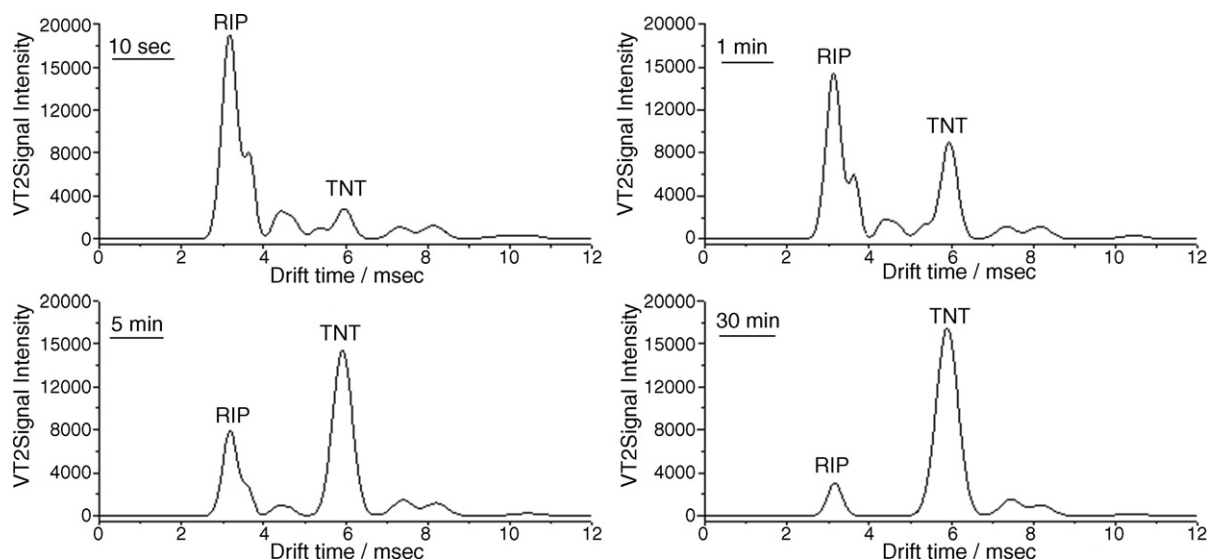


Fig. 10. Individual IMS spectra taken after 10 s, 1 min, 5 min and 30 min of TNT collection time.

data for a total of six heaters (two on each device) is presented in Fig. 5. These data were also used to calculate temperature as a function of power in Fig. 8. The individual heater curves are shown to give a sense of manufacturing uniformity.

Empirical determination of the thermal time constant, see Fig. 7, was performed using a Keithley 2400 Source Meter set to source voltage at 30 V. Triggering and data collection were controlled using a LabView™ program. Using an oscilloscope, the source meter output was found to stabilize within 4 ms and was capable of recording data points every 5 ms. Measurements were performed on a packaged device isolated in a small enclosed volume. A total of 10 measurements were averaged to produce the experimental transient data.

6. TNT detection enhancement

Experiments with a commercial ion mobility spectrometer explosives and narcotics detector (VaporTracer 2, GE Iontrack, Wilmington, MA) were performed to demonstrate the potential of the device for enhancing vapor phase detection of explosives. In these experiments, TNT vapor was generated at a constant (but uncalibrated) concentration, near saturated vapor pressure, using non-hazardous explosives for security training and testing (NESTT) material, Van Aken International, Los Angeles, CA (92% fused silica, 8% 2,4,6-TNT) packed in a thermostated column. Nitrogen flow rate and column temperature control allowed for the variation of the TNT vapor concentration.

Experiments involved setting the vapor concentration to a value near the noise floor of the detector then observing changes in the relative intensities of the reactant ions and TNT product ions when the analyte was desorbed from the preconcentrator. TNT vapor was generated with the column temperature below ambient at 18 °C in order to minimize the affects of condensation. Vapors were collected on the device at a flow rate of 400 ml/min for 15 min. This flow rate was chosen so that the TNT concentration was near the noise floor of the detector. Thus in Fig. 9, a 10 s air sample was then drawn into the detector

while the preconcentrator was desorbed producing a TNT peak with at least an order of magnitude increase in peak height. The product ion associated with TNT at a drift time of about 6.0 ms increases dramatically in intensity directly after heating the preconcentrator to desorb analyte with a concomitant loss in reactant ion intensity (drift time approximately 3.5 ms). Observing the TNT product ion over the 10 s detector sample period, the detector response to background TNT from the vapor generator is initially relatively low. It is not until the preconcentrator is desorbed and delivers the collected TNT vapor that a significant signal enhancement is achieved. It should also be noted that the TNT product ion intensity does not return to baseline after the desorption step. The incomplete clear-out of the analyte after desorbing in Fig. 9 likely resulted from cool surfaces within the flow path downstream of the preconcentrator. Unheated surfaces such as the chip package, the mounting chuck or regions on the preconcentrator may be responsible.

Fig. 10 illustrates the affect of varying the collection time of TNT vapor onto CASPAR. A single IMS spectrum is shown for the different collection times (10 s, 1 min, 5 min, 30 min). Each spectrum shows the maximum TNT product ion intensity observed when analyte is desorbed. As collection time increases so TNT product ion intensity increases on desorption. It is interesting to note the loss of proportionality between TNT peak height and time in the 5 min and 30 min spectra. Further tests indicated full saturation after ~13 min of collection suggesting either complete depletion of reactive ions or HC polymer film saturation.

7. Conclusions

Using a basic preconcentrator design, three heater support schemes were investigated; p++ silicon, silicon nitride and polyimide. Only the polyimide design proved to be both robust and capable of being produced with a reasonable yield.

A single preconcentrator plate was used with a Vapor Tracer II trace explosives detector to demonstrate a significant sensitivity

enhancement for direct TNT vapor detection. The determination of the actual sensitivity enhancement is complicated by the performance of the preconcentrator, which resulted in a signal response at or beyond the dynamic range of the detector. Given the dynamic range, in general, of IMS technology the sensitivity enhancement observed was at least one order of magnitude. The prototype preconcentrator achieved a temperature of 120 °C at ~30 V in 200 ms while consuming 175 mW in a dc drive mode.

Simulation of the average heater operating temperature as a function of voltage indicates a maximum of 7% deviation from experiment. This error is barely statistically significant given the error bars on the measurement; however the simulation might be improved by refinement of the convection coefficients. Investigating the preconcentrator's performance in vacuum where there are no convective losses can further elucidate these constants.

The relatively large deviation between experimental (121 ms) and simulated (41 ms) thermal time constants might be attributed to two shortcomings in the model. First, the power input to the hotplate is a constant in the model given that the current flowing through the heater is taken from the steady state solution. This treatment effectively reduces the average power input in the simulation during the transient period as compared to experiment. One would expect this to result in a longer modeled time constant. Second, the convection coefficients in the model are treated as constants independent of temperature and therefore time. In reality, the development of convective cells is a strong function of the device's surface temperature. This variable can be elucidated by comparing model and experiment in vacuum without convective losses.

Direct measurements of the two-dimensional thermal distribution has yet to be performed due to difficulties associated with the low emissivity of the thin polyimide membrane. However, simulation indicates up to 50 °C variation in temperature over the hotplate surface at the operating voltage of 30 V and a heater temperature of 120 °C. This problem is caused by the relatively low thermal conductivity of the polyimide layer. Future designs will incorporate a metal thermal distribution plate sputtered onto the back of the preconcentrators. A second problem is the relatively long thermal time constant indicated by the transient measurements. Future prototypes will be produced from thinner polyimide layers in an effort to reduce the thermal mass and compensate for addition of a thermal distribution plate.

Further, by stacking together multiple devices the dynamic range and collection efficiency will be improved.

Acknowledgements

We would like to thank Richard Lareau from the Transportation Security Administration and Linda Deel from the Bureau of Alcohol, Tobacco and Firearms for financial support. Thanks also to Paul Haigh and John Sperling at GE Ion Track for technical assistance and for the loan of the Vapor Tracer II detection system.

References

- [1] D. Kong, T. Mei, Y. Tao, L. Ni, T. Zhang, W. Lu, Z. Zhang, R. Wang, A MEMS sensor array for explosive particle detection, in: Proceedings of International Conference on Information Acquisition, Hefei, China, June 21–25, 2004, pp. 278–281.
- [2] T. Frisk, D. Ronnholm, W. van der Wijngaart, G. Stemme, Fast narcotics and explosives detection using a microfluidic sample interface, in: Proceedings of the Transducers '05 on the 13th International Conference on Solid-State Sensors, Actuators and Microsystems, vol. 2, Seoul, South Korea, June 5–9, 2005, pp. 2151–2154.
- [3] V.K. Pamula, R.B. Fair, Detection of nanogram explosive particles with a MEMS sensor, in: Proceedings of the SPIE on the International Society for Optical Engineering, vol. 3710, Orlando, FL, April 4–9, 1999, pp. 321–327.
- [4] J.I. Baumbach, G.A. Eiceman, Ion mobility spectrometry: arriving on site and moving beyond a low profile, *Appl. Spectrosc.* 53 (1999) 338A–355A.
- [5] G.A. Eiceman, Ion-mobility spectrometry as a fast monitor of chemical composition, *Trends Anal. Chem.* 21 (2002) 259–275.
- [6] R.G. Ewing, D.A. Atkinson, G.A. Eiceman, G.J. Ewing, A critical review of ion mobility spectrometry for detection of explosives, *Talanta* 54 (2001) 515–529.
- [7] R.P. Manginell, G.C. Frye-Mason, R.J. Kottenstette, P.R. Lewis, C. Wong, Microfabricated planar preconcentrator, in: Proceedings of the Technical Digest on Solid-State Sensor and Actuator Workshop, Hilton Head Isl, SC, Transducer Research Foundation, Cleveland, 2000, pp. 179–182.
- [8] W.-C. Tian, S.W. Pang, Thick and thermally isolated Si microheaters for microfabricated preconcentrators, *J. Vac. Sci. Technol. B* 21 (2003) 274–279.
- [9] W.-C. Tian, S.W. Pang, C.-J. Lu, E.T. Zellers, Microfabricated preconcentrator–focuser for a microscale gas chromatograph, *J. Microelectromech. Syst.* 12 (2003) 264–272.
- [10] W.C. Tian, H.K.L. Chan, C.J. Lu, S.W. Pang, E.T. Zellers, Multiple-stage microfabricated preconcentrator–focuser for micro gas chromatography system, *J. Microelectromech. Syst.* 14 (2005) 498–507.
- [11] A.M. Ruiz, I. Gracia, N. Sabate, P. Ivanov, A. Sanchez, M. Duch, M. Greboles, A. Moreno, C. Cane, Membrane-suspended microgrid as a gas preconcentrator for chromatographic applications, *Sens. Actuators A* 135 (2007) 192–196.
- [12] E.J. Houser, D.L. Simonson, J. Stepnowski, S.K. Ross, S.V. Stepnowski III, R.A. McGill, Design of hydrogen bond acidic polycarbosilanes for chemical sensor applications, *ACS Polym. Prepr.* 45 (2004) 541–542.
- [13] D. Briand, M.-A. Grettillat, B. van der Schoot, N.F. de Rooij, Thermal management of micro-hotplates using MEMCAD as simulation tool, in: Conference Proceedings of the Third International Conference on the Modeling and the Simulation of Microsystems, San Diego USA, March 27–29, 2000.
- [14] PI-2600 Process Guide Technical Bulletin, HD Microsystems, Parlin, NJ. Available at www.hdmicrosystems.com/conn/pdfform.html.

Biographies

Michael D. Martin received a BS degree in physics from Austin Peay State University in 1994 and a MS degree in physics from the University of Louisville. In 2002 he began working as a microfabrication scientist at the Microtechnology Center at University of Louisville. His research interests include development of microfabricated vapor and particle preconcentrators, trace metal detection, and devices that utilize lipid membranes.

Kevin M. Walsh received the BS and MEng degrees in electrical engineering from the University of Louisville, Louisville, Kentucky, and the PhD degree in electrical engineering (microelectronics) from the University of Cincinnati, Cincinnati, Ohio in 1978, 1985, and 1992, respectively. He is a full professor with the Electrical and Computer Engineering Department at the University of Louisville, where he also serves as the director of the UofL Micro/NanoTechnology Center and its associated 10,000 sq. ft. class 100 clean-room facility. Dr. Walsh is on the editorial board of *Sensor Letters*, has several patents and is co-founder of 3 technical start-up companies. He has taught over

20 different courses, advised over 25 completed theses, and published over 100 technical papers in the areas of micro/nanotechnology, MEMS, micro-fabrication, packaging, sensors, actuators, cleanroom design/operation, and micro/nanotechnology course development. In 2000, Prof. Walsh was inducted into the Trinity High School Hall of Fame, 2001 into the UofL Athletic Hall of Fame, and in 2005 the Kentucky Tennis Hall of Fame.

R. Andrew McGill is the head of the Functionalized Materials and Devices Section in the Sensors and Materials branch at the U.S. Naval Research Laboratory. He received a BSc (Honors) (1984) and a PhD in chemistry (1988) from the University of Surrey, England, followed by a 2 year postdoctoral position. He has worked at the Naval Research Laboratory (NRL) since 1991, and as a member of the NRL technical staff since 1995. In 1998, he formed the Functionalized Materials and Devices Section. His research interests span basic and applied areas including molecular interactions, rational materials design, synthesis of functionalized sorbent materials/polymers, microfabricated and nano devices, and chemical, biological, and explosives sensors/detectors for monitoring toxic, and hazardous materials.

Eric J Houser has a BA in chemistry from Rockford College and a PhD in inorganic chemistry from the University of Illinois. He was a postdoctoral fellow at the University of Virginia, Department of Chemistry with Professor Russell N. Grimes from 1995 to 1997. In 1997, he moved to the Naval Research Laboratory in Washington, DC where he worked in the areas of preceramic and functional polymer materials, chemical sensor system design and carbon

nanotube devices for the detection of chemical weapons and explosives. In 2005, he accepted a position at the Transportation Security Laboratory in Atlantic City, NJ where he works in the area of trace explosives detection.

Jennifer Stepnowski received a BS degree in chemistry (with a minor in mathematics) from The George Washington University, Washington, DC, in 1996, and a MS degree in physical chemistry from the University of California at San Diego, La Jolla, in 1999. She is currently a research chemist with Nova Research, Inc., working in the Functionalized Materials and Devices Section of the U.S. Naval Research Laboratory (NRL), Washington, DC. She has a wide range of experience in the following areas: development of sensor systems, fabrication and characterization of sorbent-coated microfabricated structures, testing of sensors and detectors, evaluation of commercial detectors, and development and calibration of vapor delivery systems.

Stanley Stepnowski received the BSEE degree from The George Washington University, Washington, DC, in 1997. From 1991 to 1992, he was an electronics technician with the Naval Nuclear Power Program of the U.S. Navy. He was also a Surface Warfare Officer aboard ships in operations and combat systems departments. In 2001, he joined the U.S. Naval Research Laboratory (NRL), Washington, DC, where he has developed prototype sensor systems including analog interface electronics design and microcontroller programming and is currently the lead electrical engineer with the Functionalized Materials and Devices Section. Mr. Stepnowski was a co-recipient of the 2004 R&D 100 Award for his work on microcantilevers for explosives detection.